

# Interface quality and thermal stability of laser-deposited metal/MgO multilayers

Christian Fuhse, Hans-Ulrich Krebs, Satish Vitta, and Göran A. Johansson

Metal/MgO multilayers (metal of Fe, Ni<sub>80</sub>Nb<sub>20</sub>, and Ti) with bilayer periods in the range 1.2–3.0 nm have been prepared by pulsed laser deposition and characterized by both hard and soft-x-ray reflectometry. The interface roughness is found to be  $\leq 0.5$  nm in all the samples and is nearly independent of the total number of deposited bilayers. The interface roughness, however, depends on the absolute thickness of the individual layers and increases from  $\approx 0.3$  nm for a 3.0-nm period to  $\approx 0.5$  nm for a bilayer period of 1.2 nm. The multilayers are found to be highly stable up to temperatures as high as 550 °C. The hard-x-ray reflectivity of the multilayers decreases for  $T > 300$  °C, whereas the layered structure is stable up to 550 °C. The reflectivity in the water window region of soft x rays,  $\lambda = 3.374$  nm, was found to be 0.4% at an angle of incidence of  $\approx 54^\circ$  for multilayers with 60 bilayers at a period of  $\approx 2.1$  nm. © 2004 Optical Society of America

OCIS codes: 230.4170, 340.7470, 310.0310, 310.3840, 340.0340.

## 1. Introduction

The physical properties of multilayers with individual layer thicknesses in the nanometer range depend critically on the nature of the interfaces. Hence a study of interface roughness and its development becomes highly significant. In particular, the reflectivity of multilayer mirrors is attenuated by interface roughness,<sup>1</sup> which has two distinct components—morphological roughness and intermixing. In the case of vapor-phase condensation, the morphological roughness depends on the surface mobility of the condensing particles, a function of their energy, and the rate of deposition. The condensing particles should have sufficient energy for surface movement to form a smooth surface. An excess energy for the condensing particles on the other hand can lead to implantation or intermixing.<sup>2</sup> Hence control of the energy of the condensing particles becomes crucial for the deposition of multilayers with smooth interfaces, and

pulsed laser deposition becomes a suitable technique for this purpose. Pulsed laser deposition offers the additional advantage of stoichiometric transfer of both alloys and oxides. Hence this technique has been used in the present study to prepare multilayers for the water window region of soft x rays ( $\lambda = 2.3$ – $4.4$  nm). The stability of multilayers and the interface roughness depend on interdiffusion between individual components, and this has to be minimized to maximize the thermal and temporal stability.

The selection of materials for the multilayer constituents in the present study is done based on the dual purpose of water window soft-x-ray mirrors and by maximization of the thermal and temporal stability. One of the suitable spacer elements for the water window region is Mg. However, since it is highly unstable and reactive, the more stable MgO has been used as spacer material together with absorbers Ni<sub>80</sub>Nb<sub>20</sub> and Fe. A survey of the optical constants of various materials indicates that Ti is an excellent spacer for wavelengths slightly above that of its L-absorption edge at  $\lambda = 2.73$  nm. In this case MgO becomes the absorber. We determined the interface quality using both hard and soft x rays. The thermal stability of the multilayers up to 600 °C in an ultrahigh-vacuum (UHV) environment has been investigated by hard-x-ray reflectivity.

## 2. Experimental Methods

All the multilayers were deposited at room temperature in an UHV chamber (base pressure  $< 10^{-8}$

---

C. Fuhse (cfuhse@uni-goettingen.de) and H.-U. Krebs (krebs@ump.gwdg.de) are with the Institut für Materialphysik, Universität Göttingen, Tammanstrasse 1, Göttingen 37077, Germany. S. Vitta (satish.vitta@iitb.ac.in) is with the Department of Metallurgical Engineering and Materials Science, Indian Institute of Technology, Bombay, Mumbai 400076, India. G. A. Johansson is with Biomedical and X-Ray Physics, Department of Physics, Royal Institute of Technology, Stockholm 106 91, Sweden.

Received 19 January 2004; accepted 2 April 2004.

0003-6935/04/346265-05\$15.00/0

© 2004 Optical Society of America

**Table 1. Fit Parameters of the Hard-X-Ray Reflectivity Curves Shown in Figs. 1–3 Performed on Samples Consisting of Metal and MgO Bilayers**

Sample	$N^a$	$\Lambda$ (nm) <sup>b</sup>	$\sigma$ (nm) <sup>c</sup>	$\Gamma^d$
Ni <sub>80</sub> Nb <sub>20</sub> /MgO (Fig. 1)				
(a)	40	2.36	0.35	0.70
(b)	40	2.18	0.35	0.50
(c)	40	1.46	0.52	0.33
(d)	40	1.38	0.51	0.30
(e)	40	1.19	0.50	0.50
Fe/MgO (Fig. 2)				
(a)	20	2.20	0.33	0.38
(b)	55	2.11	0.35	0.37
(c)	65	2.14	0.40	0.21
Ti/MgO (Fig. 3)				
(a)	36	1.50	0.20	0.50
(b)	38	1.35	0.33	0.50

<sup>a</sup> $N$ , number of bilayers.<sup>b</sup>Multilayer period.<sup>c</sup>rms roughness.<sup>d</sup>Ratio of metal layer thickness to bilayer period.

mbar). For deposition, a KrF excimer laser (wavelength 248 nm, pulse duration 30 ns, pulse energy 110 mJ, repetition rate 3–10 Hz) was focused onto an area of approximately 2 mm<sup>2</sup> leading to an energy density of  $\approx 5.5$  J/cm<sup>2</sup> on the targets (Fe, Ni<sub>80</sub>Nb<sub>20</sub>, Ti, and MgO).

The substrates were cut from standard Si (111) and (001) single-crystal wafers with a native surface oxide layer. The multilayers deposited on the two types of substrate did not show any difference in the crystalline orientation or in the interface roughness, indicating that the substrate orientation does not influence the structure of the deposited film. Hence no reference is made to the crystallographic orientation of the substrate in our discussion of the results. The multilayers were deposited with MgO as the first layer on the substrate and a metal layer as the top layer.

We carried out the hard-x-ray reflectivity measurements with a Philips X'Pert diffractometer using Co K $\alpha$  ( $\lambda = 0.179$ -nm) radiation. We studied the thermal stability of the multilayers by annealing for 75 min in the temperature range of 200 °C to 600 °C in the UHV environment. The structure following each annealing was determined by hard-x-ray reflectometry. The reflectivity in the water window region,  $\lambda = 3.374$  nm, was measured for selected multilayers with a soft-x-ray reflectometer based on a line-emitting laser-plasma source as described by Johansson *et al.*<sup>3</sup>

### 3. Results and Discussion

#### A. Hard-X-Ray Reflectivity

The structure of all the multilayers was first characterized by hard-x-ray measurements (see Figs. 1–3). The reflectivity scans show clear total thickness oscillations (Kiessig fringes) and sharp multilayer Bragg peaks indicating the presence of a well-ordered layered structure. The bilayer period  $\Lambda$  of the mul-

tilayers can be determined from the angular position of the Bragg peaks. To determine the other structural parameters such as the individual layer thickness and the interface roughness  $\sigma$ , the reflectivity has to be simulated by standard optical formalism. In the present study we performed the reflectivity simulation using IMD software<sup>4</sup> assuming a Gaussian distribution of interface height fluctuations. The height fluctuations of the two interfaces are assumed to be identical, which means that the roughness of the two interfaces will be the same. The individual layers in the multilayer are assumed to have bulk densities, and the top metal layer is assumed to be oxidized. The results of the simulations that are the best fit to experimental reflectivity data are given in Table 1 and shown in Figs. 1–3 for all the different multilayers.

The experimental hard-x-ray reflectivity curves together with the best-fit simulations for the Ni<sub>80</sub>Nb<sub>20</sub>/MgO multilayers are shown in Fig. 1. The bilayer period varies from 1.19 to 2.36 nm. The presence of clear first-order Bragg peaks even for a period of 1.19 nm shows that pulsed laser deposition can be used effectively for the deposition of ultrathin layers. The interface roughness  $\sigma$  is  $\leq 0.5$  nm in all cases. The sharp Bragg peak with a low width indicates a high correlation of roughness at all the interfaces and a roughness that is independent of the total number of bilayers in the multilayer. The simulated curves yield interface roughnesses increasing from 0.35 nm for  $\Lambda = 2.4$  nm to 0.5 nm for  $\Lambda = 1.2$  nm. Furthermore, metal layer thickness to bilayer period ratios ( $\Gamma$ ) between 0.3 and 0.7 are determined (Table 1).

The dependence or independence of  $\sigma$  on the number  $N$  of deposited bilayers was studied systematically in Fe/MgO multilayers. The bilayer period  $\Lambda$  was kept nearly constant between 2.1 nm and 2.2 nm, and the number of deposited bilayers increased from

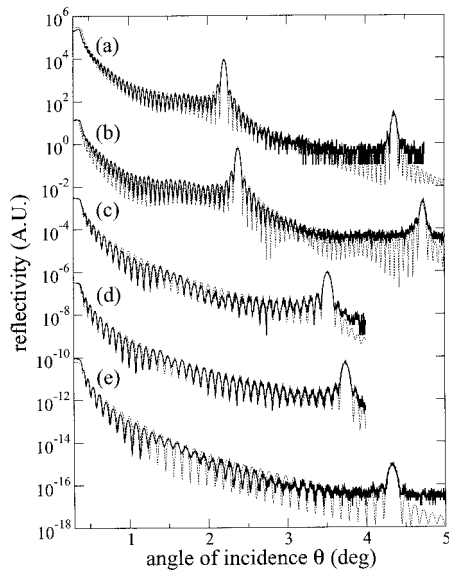


Fig. 1. Hard-x-ray reflectivity of  $\text{Ni}_{80}\text{Nb}_{20}/\text{MgO}$  multilayers as a function of the bilayer period varied in the range from of 2.36 to 1.19 nm, [(a)–(e)] showing clear total thickness oscillations and the layer period Bragg peak (solid curves). The number of bilayers is kept constant at 40. A simulation of the reflectivity (dashed curves) gives the interface roughness variation with the period. The curves are shifted vertically for clarity.

20 to 65. The reflectivity curves together with the simulations are shown in Fig. 2. The interface roughness determined from the simulations increases only slightly from 0.33 to 0.40 nm when the number of bilayers increases from 20 to 65 (see Table 1). These results clearly show that  $\sigma$  does not scale with  $N$  and reaches a saturation. In the case of Ti/MgO multilayers, (Fig. 3), the interface roughness is found to be even lower than in Fe/MgO and  $\text{Ni}_{80}\text{Nb}_{20}/\text{MgO}$  multilayers. The value of  $\sigma$  in 1.35-nm period Ti/MgO multilayers is  $\approx 0.33$  nm whereas for a comparable  $\text{Ni}_{80}\text{Nb}_{20}/\text{MgO}$  multilayer with a period of 1.38 nm the interface roughness is

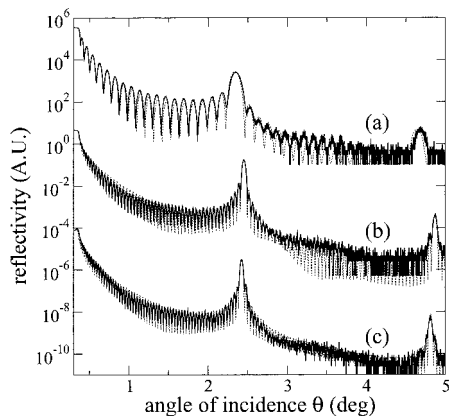


Fig. 2. Hard-x-ray reflectivity of Fe/MgO multilayers as a function of varying number: (a) 20, (b) 55, and (c) 65. Periods between 2.1 and 2.2 nm show clear peaks and hence a complete layer ordering. The results of our simulations (dashed curves) are also shown. The curves are shifted vertically for clarity.

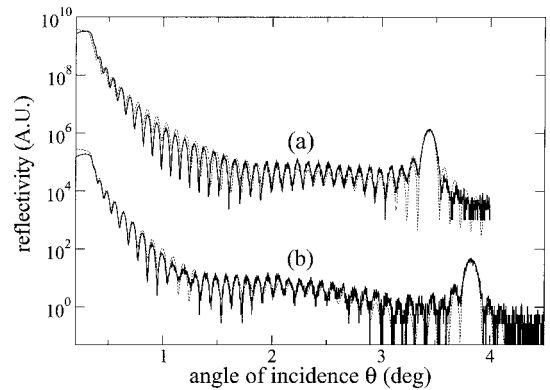


Fig. 3. Measured (solid curves) and simulated (dashed curves) hard-x-ray reflectivity of Ti/MgO multilayers with (a) 1.50-nm and (b) 1.35-nm periods. A simulation of reflectivity shows that the interface roughness is 0.20 and 0.33 nm, respectively. The curves are shifted vertically for clarity.

$\approx 0.50$  nm. These results show that the growth behavior of Ti is different compared with Fe or  $\text{Ni}_{80}\text{Nb}_{20}$ .

A comparison of the interface roughness values for the multilayers given in Table 1 shows that  $\sigma$  increases with decreasing  $\Lambda$  (see Fig. 4). This behavior is contrary to the growth behavior observed by Mertins *et al.*<sup>5</sup> and Schäfers *et al.*<sup>6</sup> who grew the multilayers using a sputtering technique. It can be concluded from the present observations that an ultrathin-film growth mechanism in UHV pulsed laser deposition is very different from that in sputter deposition.

#### B. Soft-X-Ray Reflectivity

The soft-x-ray reflectivity of typical  $\text{Ni}_{80}\text{Nb}_{20}/\text{MgO}$  and Fe/MgO multilayers was measured at a wavelength of 3.374 nm provided by a line-emitting laser-plasma source. Since this wavelength is not ideal for Ti-based multilayers (the L-absorption edge is at 2.73 nm), the soft-x-ray reflectivity of these multilayers was not measured. Figure 5 shows the reflectivity of a 60-bilayer, 2.11-nm period  $\text{Ni}_{80}\text{Nb}_{20}/\text{MgO}$

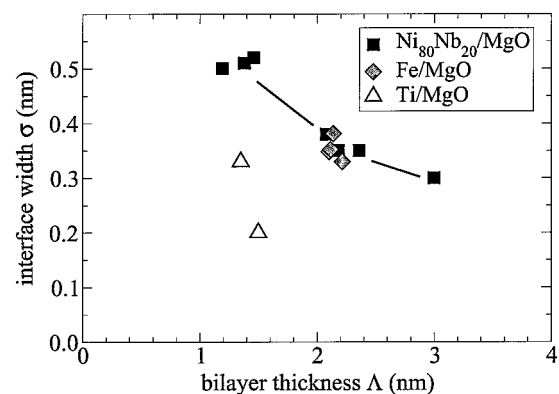


Fig. 4. Summary of the rms interface roughness values  $\sigma$  measured on  $\text{Ni}_{80}\text{Nb}_{20}/\text{MgO}$ , Fe/MgO, and Ti/MgO multilayers with bilayer period  $\Lambda$ .

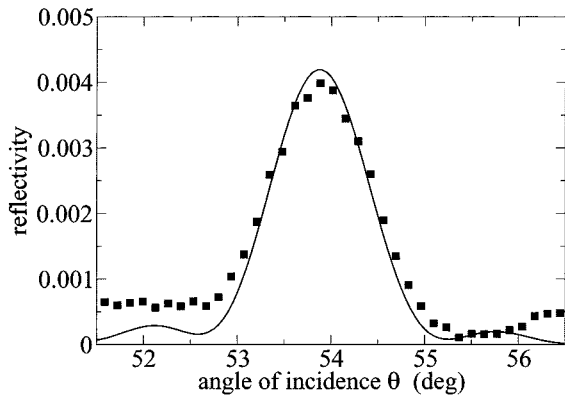


Fig. 5. Soft-x-ray reflectivity of a 60-bilayer, 2.11-nm period  $\text{Ni}_{80}\text{Nb}_{20}/\text{MgO}$  multilayer at  $\lambda = 3.374$  nm. The solid curve represents the simulation to the measured data shown as squares.

multilayer, and the reflectivity of a 65-bilayer, 2.14-nm period  $\text{Fe}/\text{MgO}$  multilayer is shown in Fig. 6. The absolute reflectivity in both cases is found to be  $\approx 0.4\%$ , a relatively high value considering that the individual layers' thickness was not optimized and that there were only approximately 60 bilayer pairs.

### C. Thermal Stability

The usability of multilayers for any application depends on their stability with respect to temperature and time. Hence the thermal stability of typical  $\text{Ni}_{80}\text{Nb}_{20}/\text{MgO}$  and  $\text{Fe}/\text{MgO}$  multilayers in the range  $200^\circ\text{C}$ – $600^\circ\text{C}$  has been studied with hard-x-ray reflectivity. The results of annealing for 75 min at different temperatures are shown in Figs. 7 and 8.

The results show that both types of multilayer are highly stable up to temperatures of  $\approx 550^\circ\text{C}$ . The layered structure can be clearly seen by the well-defined first-order Bragg peaks. The bilayer Bragg peaks vanish after annealing at  $600^\circ\text{C}$ , revealing severe interdiffusion and roughening leading to a breakdown of the layered structure. The position and height of the first-order Bragg peak changes when annealed at temperatures in the range  $200^\circ\text{C}$ – $300^\circ\text{C}$ . The bilayer period is found to decrease

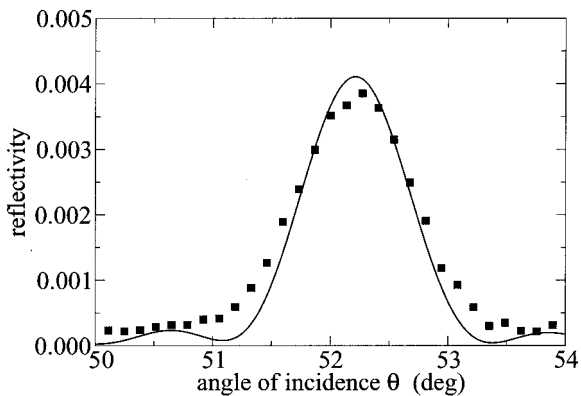


Fig. 6. Soft-x-ray reflectivity of a 65-bilayer, 2.14-nm  $\text{Fe}/\text{MgO}$  multilayer at  $\lambda = 3.374$  nm. The solid curve represents the simulation to the measured data shown as squares.

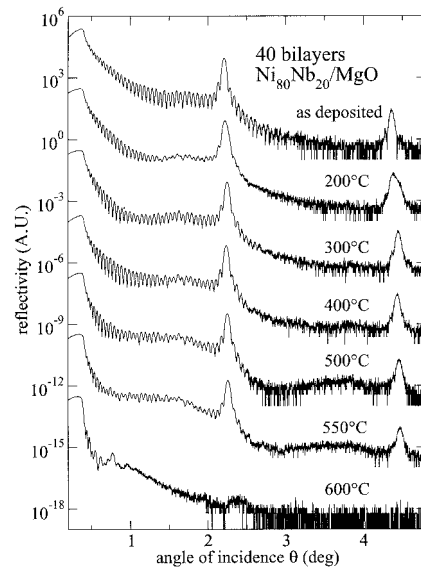


Fig. 7. Thermal stability of 2.4-nm period  $\text{Ni}_{80}\text{Nb}_{20}/\text{MgO}$  multilayers in the temperature range  $200^\circ\text{C}$ – $600^\circ\text{C}$  is studied by hard-x-ray reflectivity. The multilayers were annealed for 75 min at each temperature and cooled to room temperature before the reflectivity was measured. The curves are shifted vertically for clarity.

slightly, 1%–2%, and the first-order Bragg peak reflectivity increases compared with the as-deposited state (Fig. 7). These results are in agreement with the results of Vitta and Yang,<sup>7</sup> where improved reflectivity was found after annealing  $\text{Ni-Nb}/\text{C}$  multilayers due to atomic relaxation processes. Although the layered structure is present till  $550^\circ\text{C}$ , the reflectivity decreases for  $T > 300^\circ\text{C}$ , as can be seen in Fig.

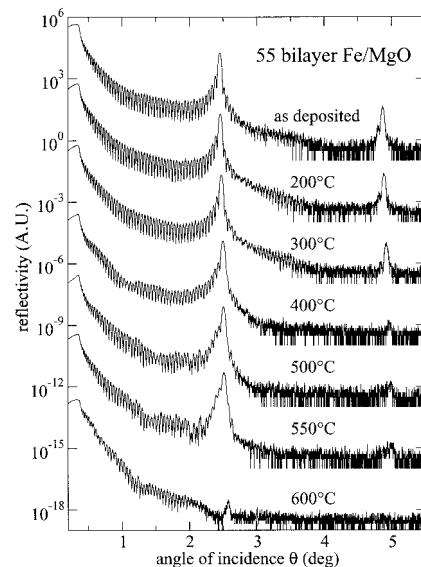


Fig. 8. Thermal stability of 2.1-nm period  $\text{Fe}/\text{MgO}$  multilayers in the temperature range  $200^\circ\text{C}$ – $600^\circ\text{C}$  is studied by hard-x-ray reflectivity. The multilayers were annealed for 75 min at each temperature and cooled to room temperature before the reflectivity was measured. The curves are shifted vertically for clarity.

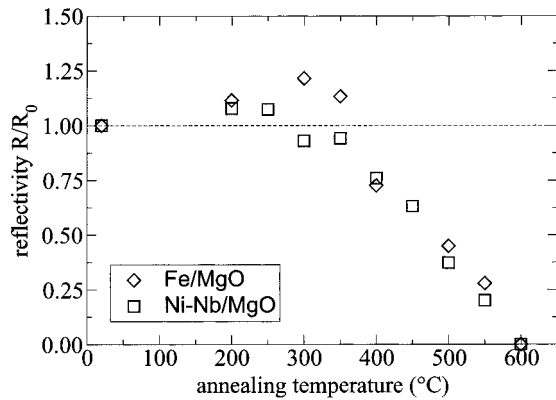


Fig. 9. Effect of annealing at different temperatures is studied by the monitoring of the first-order Bragg peak reflectivity with respect to the as-deposited multilayer. The reflectivity drops for  $T > 300$  °C and the layered structure breaks down at 600 °C.

9, indicating this to be the onset temperature for severe interdiffusion and roughening.

#### 4. Conclusion

Three different types of multilayer mirrors for the water window soft-x rays with two different absorber and spacer combinations have been made with periods in the range of 1.19–2.36 nm. In the case of  $\text{Ni}_{80}\text{Nb}_{20}/\text{MgO}$  and  $\text{Fe}/\text{MgO}$  multilayers, MgO is the spacer; and in the  $\text{Ti}/\text{MgO}$  multilayers, it acts as the absorber because of its optical constants in comparison with  $\text{Ni}_{80}\text{Nb}_{20}$ , Fe, and Ti.

The interface roughness increases with a decreasing period and is found to be  $\leq 0.5$  nm even in the lowest period multilayer. This is due to the deposition process that provides sufficient energy for the condensing particles to move freely on the surface to smoothen it but not enough to lead to intermixing.

The low roughness results in a relatively high soft-x-ray reflectivity at high angles of incidence. Optimizing the absorber and spacer thickness can lead to significant improvements in soft-x-ray reflectivity.

The  $\text{Ni}_{80}\text{Nb}_{20}/\text{MgO}$  and  $\text{Fe}/\text{MgO}$  multilayers have a very high thermal and temporal stability as can be seen from the annealing results. The layered structure is stable even after annealing for 75 min at 550 °C. This is due to the lack of an interdiffusion potential between the ceramic MgO layers and the respective metal layers. MgO is highly stable and can only undergo roughening with very little interdiffusion. This suggests that the multilayers with MgO as one of the constituents can take substantial heat load even when used with intense synchrotron radiation.

#### References

1. A. G. Michette, "X-ray microscopy," *Rep. Prog. Phys.* **51**, 1525–1606 (1988).
2. K. Sturm and H.-U. Krebs, "Quantification of resputtering during pulsed laser deposition," *J. Appl. Phys.* **90**, 1061–1063 (2001).
3. G. A. Johansson, M. Berglund, F. Eriksson, J. Birch, and H. M. Hertz, "Compact soft x-ray reflectometer based on a line-emitting laser plasma source," *Rev. Sci. Instrum.* **72**, 58–62 (2001).
4. D. L. Windt, "IMD—software for modeling the optical properties of multilayer films," *Comput. Phys.* **12**, 360–370 (1998).
5. H.-C. Mertins, F. Schäfers, H. Grimmer, D. Clemens, P. Böni, and M. Horisberger, "W/C, W/Ti, Ni/Ti, and Ni/V multilayers for the soft-x-ray range: experimental investigation with synchrotron radiation," *Appl. Opt.* **37**, 1873–1882 (1998).
6. F. Schäfers, H.-C. Mertins, F. Schmolla, I. Packe, N. N. Salashchenko, and E. A. Shamov, "Cr/Sc multilayers for the soft-x-ray range," *Appl. Opt.* **37**, 719–728 (1998).
7. S. Vitta and P. Yang, "Thermal stability of 2.4 nm period Ni-Nb/C multilayer x-ray mirror," *Appl. Phys. Lett.* **77**, 3654–3656 (2000).